Neuroimage: Reports 6 (2026) 100311

Contents lists available at ScienceDirect

Neuroimage: Reports

journal homepage: www.sciencedirect.com/journal/neuroimage-reports

Neural and biomarker correlates of the Parkinson's Disease–Cognitive Rating Scale in Huntington's disease

Saul Martinez-Horta [a,b,c,d,e], Arnau Puig-Davi [a,b,c,d,e], Frederic Sampedro [f], Jesús Pérez-Pérez [a,b,c,d,e], Carla Franch-Martí [a,b,c,e], Gonzalo Olmedo-Saura [a,b,c,d,e], Elisa Rivas-Asensio [a,b,c,d,e], Anna Vazquez-Oliver [a,b,c,d,e], Laura Pérez-Carasol [a,b,c,d,e], Andrea Horta-Barba [a,b,c,d,e], Javier Pagonabarraga [a,b,c,d,e], Jaime Kulisevsky [a,b,c,d,e,*]

[a] Movement Disorders Unit, Neurology Department, Hospital de la Santa Creu i Sant Pau, Barcelona, Spain
[b] Research Institute Sant Pau (IR-Sant Pau), Barcelona, Spain
[c] Centro de Investigación Biomédica en Red-Enfermedades Neurodegenerativas (CIBERNED), Spain
[d] Department of Medicine. Autonomous University of Barcelona), Spain
[e] European Huntington's Disease Network (EHDN), Spain
[f] Neuroradiology Department, Hospital Vall d'Hebron - Institut de Diagnostic per la Imatge, Barcelona, Spain

ARTICLE INFO

Keywords:
Huntington's disease
PD-CRS
Cognitive assessment
MRI
Neuropsychology

ABSTRACT

Background: Cognitive decline is a core feature of Huntington's disease (HD), often preceding motor symptoms and progressing with disease severity. While several neuropsychological tests track cognitive changes, few studies have examined the biological correlates of brief screening tools adapted for HD.
Objectives: This study investigates the neuroanatomical and fluid biomarker correlates of performance on the Parkinson's Disease–Cognitive Rating Scale (PD-CRS), aiming to validate it as a clinically and biologically grounded tool for cognitive assessment in HD.
Methods: Fifty-two symptomatic gene-expansion carriers (CAG >39) underwent cognitive (PD-CRS), motor (UHDRS), and behavioral (PBA) assessments. Plasma neurofilament light chain (NfL) levels were measured via Simoa as a marker of neurodegeneration. Voxel-based morphometry (VBM) was used to identify gray matter volume (GMV) correlates of PD-CRS scores. Linear regressions evaluated relationships among PD-CRS, GMV, and NfL, including subdomain-level and stage-stratified analyses based on HD-ISS classification.
Results: PD-CRS scores were significantly associated with GMV in frontostriatal, paralimbic, parietal, and occipital regions. NfL levels correlated with both cognitive scores and GMV in key regions, supporting their value as biomarkers of neurodegeneration. Subdomain analyses revealed region-specific associations (e.g., visuospatial tasks with posterior cortices, fluency with striatum). Perseveration, motor severity, and education predicted PD-CRS performance (adjusted $R^2 = 0.799$). PD-CRS remained the strongest GMV predictor (adjusted $R^2 = 0.519$), particularly in later disease stages.
Conclussions: The PD-CRS reflects biologically meaningful aspects of cognitive dysfunction in HD, with robust associations to structural and molecular disease markers. These findings support its use as a practical and sensitive tool for clinical and research applications.

1. Introduction

Huntington's disease (HD) is a neurodegenerative disorder caused by an abnormal expansion of CAG trinucleotide repeats in the HTT gene on chromosome 4[1]. This mutation triggers a cascade of progressive neuropathological changes, ultimately leading to neuronal dysfunction and death, particularly in the striatum, although widespread involvement of cortical regions and white matter is also observed (Ross and Tabrizi, 2011; Rosas et al., 2008; Adanyeguh et al., 2021).

Cognitive decline is a core feature of HD, typically emerging years

* Corresponding author. Movement Disorders Unit, Neurology Department, Hospital de la Santa Creu i Sant Pau, Mas Casanovas 90, 08041, Barcelona, Spain.
E-mail address: jkulisevsky@santpau.cat (J. Kulisevsky).

https://doi.org/10.1016/j.ynirp.2025.100311
Received 28 October 2025; Received in revised form 27 November 2025; Accepted 12 December 2025

before the onset of motor symptoms (Snowden, 2017). This decline follows a predominantly fronto-striatal pattern, progressively affecting multiple cognitive domains and culminating in a dementia syndrome (Martinez-Horta et al., 2023). While features such as psychomotor slowing, attentional deficits, and frontal-dysexecutive dysfunction are prominent, the cognitive phenotype of HD is heterogeneous, both in terms of domain involvement and progression trajectory across individuals (Snowden, 2017; Martinez-Horta et al., 2023; Horta-Barba et al., 2023; Sierra et al., 2023).

Longitudinal studies have shown that tests like the Symbol Digit Modalities Test (SDMT) and Stroop Word Reading are sensitive to cognitive changes in HD (Tabrizi et al., 2012; Schobel et al., 2017). While useful as markers of disease progression, they provide limited information on patients' overall cognitive status (Martinez-Horta et al., 2020a; Mestre et al., 2018). Although not a replacement for full neuropsychological assessment, screening tools offer a practical, time-efficient way to detect cognitive impairment and they are particularly valuable in longitudinal studies and clinical trials, where consistent and reproducible measures are crucial for tracking change and comparing outcomes (Litvan et al., 2012; Marras et al., 2014; Reber et al., 2021).

Several screening instruments have been employed in HD (Begeti et al., 2013; Folstein et al., 1975; Group, 1996; Rosca and Simu, 2022; Rosen et al., 1984; Rosser and Hodges, 1994; Stout et al., 2014). However, a systematic review of these tools concluded that none currently fulfil the criteria for general recommendation in HD (Mestre et al., 2018). In response to this gap, our group conducted a series of studies evaluating the Parkinson's Disease - Cognitive Rating Scale (PD-CRS) in the context of HD (Horta-Barba et al., 2023; Martinez-Horta et al., 2020a, 2020b). These investigations demonstrated the tool's strong psychometric properties, its ability to differentiate between cognitive states, and its sensitivity to longitudinal changes, suggesting its potential as a viable screening instrument for global cognitive assessment in HD (Horta-Barba et al., 2023; Martinez-Horta et al., 2020a).

Beyond psychometric validation, identifying the neuroanatomical correlates of cognitive screening tool performance is key to linking test scores with brain pathology. However, few studies have examined the structural correlates of such tools in HD, limiting efforts to biologically ground their clinical use. To address this, we investigate the neuroanatomical correlates of PD-CRS performance in individuals with HD. Using voxel-based morphometry (VBM), we examine associations between PD-CRS scores and regional gray matter volume (GMV) in a well-characterized cohort. We also assess plasma neurofilament light chain (NfL) levels in relation to cognition and brain atrophy. By combining imaging and fluid biomarkers, we aim to validate the PD-CRS as both a clinically useful screening tool and a marker of disease-related neurodegeneration.

2. Methods

2.1. Participants

Fifty-two symptomatic gene-expansion carriers (CAG >39) were recruited from the Movement Disorders Unit at Hospital de la Santa Creu i Sant Pau (Barcelona). Demographic and clinical data were recorded. Motor severity was assessed via the UHDRS Total Motor Score (UHDRS-TMS), and functional status via the Total Functional Capacity (TFC) and Functional Independence Scale (FIS)(Group, 1996). Neuropsychiatric symptoms were evaluated using the Problem Behaviors Assessment-Short Form (PBA-s), using the product of frequency and severity scores (Callaghan et al., 2015).

Participants were classified into HD-ISS stages 1–3 based on biological criteria (Tabrizi et al., 2022). Stage 0 individuals were excluded, as they show no detectable neuropathology. Stage 1 participants were included despite being premanifest, given biomarker evidence of early neurodegeneration. Cumulative CAG-related disease burden was estimated using the CAP score: age × (CAG - 33.66) (Warner et al., 2022).

Exclusion criteria included other neurological/psychiatric disorders, traumatic brain injury with loss of consciousness, uncontrolled medical illness, active substance abuse, or psychosis. Patients unable to understand or perform study tasks were also excluded.

2.2. Cognitive assessment

Cognitive functioning was evaluated in all participants using the PD-CRS (Pagonabarraga et al., 2008). Previous work from our group has validated the PD-CRS as a sensitive tool for staging cognitive impairment in HD, distinguishing between normal cognition, mild cognitive impairment (MCI), and dementia. The PD-CRS is composed of nine subtests assessing immediate verbal memory, confrontation naming, sustained attention, verbal working memory, unprompted clock drawing, clock copy, delayed free recall, alternating verbal fluency, and action verbal fluency. The posterior–cortical subscore (range 0–30) is derived from confrontation naming and the clock copy task, while the remaining subtests contribute to the frontal–subcortical subscore (range 0–104). The sum of all subtests yields the total score, which ranges from 0 to 134, with higher scores indicating better cognitive performance. The PD-CRS A total score of ≤82 optimally identifies MCI, typically associated with minimal functional impact, while a score of ≤64 indicates dementia-level impairment with significant loss of autonomy. These thresholds have been empirically linked to functional outcomes, supporting the PD-CRS as both practical and clinically relevant for monitoring cognitive decline in HD (Horta-Barba et al., 2023; Martinez-Horta et al., 2020a).

2.3. Neuroimaging acquisition and preprocessing

High-resolution T1-weighted MRI images were obtained on a 3T Philips Achieva scanner using an MPRAGE sequence (TR/TE = 12.65/7.08 ms, flip angle = 8°, field of view = 23 cm, matrix = 256 × 256, slice thickness = 1 mm). Standard VBM procedures were performed using the SPM12 software package. (http://www.fil.ion.ucl.ac.uk/spm). GMV tissue probability maps were generated from the T1-weighted scans and subsequently normalized to the Montreal Neurological Institute (MNI) space using the DARTEL algorithm. To account for inter-individual variability, the normalized GMV maps were smoothed with an isotropic Gaussian filter with a full-width at half-maximum (FWHM) of 8 mm in all dimensions.

2.4. Biosample collection and processing

Peripheral blood samples were collected into EDTA tubes, centrifuged (2000×*g*, 10 min), and plasma was aliquoted and stored at −80 °C per international guidelines. Plasma NfL levels were measured using the Simoa® Human NF-light Advantage Kit (Quanterix) on the SR-X™ system, following the manufacturer's protocol. Calibration standards, quality controls, and duplicate samples were run on a 96-well plate. After incubation with antibody-coated beads and biotinylated detection antibodies, SBG enzyme and RGP substrate were added. Fluorescent signals were detected and quantified using a four-parameter logistic curve. All samples were analyzed in duplicate; intra-assay CVs remained below 20 %.

2.5. Statistical analysis

Descriptive statistics were computed to summarize sociodemographic, clinical, cognitive, and behavioral characteristics. Continuous variables were expressed as means and standard deviations, while categorical variables were summarized as frequencies and percentages. Group comparisons across HD-ISS stages were performed using one-way analyses of variance (ANOVA) for normally distributed variables,

followed by Tukey's HSD post hoc tests to identify specific between-group differences. For pairwise comparisons where homogeneity of variance was violated, Welch's t-tests were applied. Normality assumptions were evaluated via Shapiro-Wilk tests and visual inspection of histograms and Q-Q plots. Test statistics (F or t), degrees of freedom, p-values, and effect sizes (Cohen's d) were reported as appropriate.

Cognitive staging was based on PD-CRS total score thresholds, classifying participants as cognitively normal, mildly impaired (PD-CRS $\leq$82), or demented (PD-CRS $\leq$64)7,11. To assess relative performance across PD-CRS subdomains, raw scores were standardized into z-scores, which were calculated using the mean and standard deviation of the internal study cohort. This within-cohort normalization accounted for differing scoring ranges across subtests (e.g., action fluency max = 30 vs. clock drawing max = 10), thereby enabling direct item-level comparisons and clearer identification of the domains most sensitive to disease-related cognitive decline.

Multiple linear regression analyses were conducted to identify clinical and behavioral predictors of global cognitive performance controlling for potential confounders. Standardized beta coefficients (B), associated p-values, and R^2 values were reported. To investigate structural correlates of cognitive function, GMV maps from VBM analyses were included in a general linear model (GLM). Two analytical frameworks were implemented according to the primary target of inference: (i) PD-CRS total scores were modelled as the dependent variable when assessing the contribution of motor severity, perseverative behaviours and demographic variables to cognitive performance; and (ii) regional GMV from VBM-derived clusters was modelled as the dependent variable when assessing neuroanatomical correlates of cognitive impairment. Accordingly, PD-CRS served as predictor or outcome depending on the objective of each model. Additionally, exploratory stage-stratified analyses of the VBM-derived clusters were conducted across HD-ISS stages 1–3. Whole-brain VBM analyses applied cluster-level family-wise error (FWE) correction ($p < 0.05$) using random field theory (RFT) in SPM12. Stage-stratified and ROI-based analyses were considered exploratory given the limited subgroup sample sizes, and therefore effect sizes and spatial consistency were emphasized over additional multiple-comparison correction. GMV values from significant clusters were extracted for follow-up regressions with relevant clinical measures and PD-CRS subdomains.

Finally, multiple regression models assessed the relationship between plasma NfL concentrations and both regional GMV and PD-CRS total scores. Age was included as a covariate to account for known age-related effects on NfL. Results were reported with corresponding B values, p-values, and R^2 statistics. For visualization, VBM maps were thresholded at an uncorrected level of $p < 0.0001$ (cluster extent $k = 20$ voxels).

The study protocol was reviewed and approved by the institutional ethics committee. Written informed consent was obtained from all participants prior to their inclusion in the study. All procedures were carried out in accordance with the ethical standards of the 1964 Declaration of Helsinki and its later amendments. The data supporting the findings of this study are available from the corresponding author upon reasonable request.

3. Results

3.1. Sociodemographic and clinical characteristics

The total sample comprised 52 symptomatic gene-expansion carriers (53.8 % female) with an average of 43.9 (3.5) CAG repeats and a mean CAP score of 500.6 (89.8). Motor and functional assessments revealed a mean UHDRS-TMS score of 36.8 (21.4), a TFC score of 10.3 (2.6), a FAS score of 21.0 (3.8), and a composite Unified Huntington's Disease Rating Scale score (cUHDRS) score of 9.3 (4.8).

PD-CRS total score was 79.7 (19.1), with subcortical and cortical subscores averaging 52.7 (16.2) and 27.0 (3.3), respectively. Based on established cut-off scores, 30 participants (57.7 %) scored $\leq$82, indicating cognitive impairment consistent with mild cognitive impairment (MCI), while 10 participants (19.2 %) scored $\leq$64, consistent with dementia-level impairment. Among participants in HD-ISS stage 1, all 10 (100 %) exhibited normal cognitive status. In stage 2, 4 individuals (44.4 %) met criteria for MCI and 1 (11.1 %) for dementia. In contrast, in stage 3, 16 participants (48.5 %) fell within the MCI range and 8 (24.2 %) met the threshold for dementia. Table 1 summarizes the main clinical and sociodemographic characteristics of the sample (See Supplementary Table 1 for all clinical and sociodemographic data).

Using PD-CRS z-scores to allow direct comparison across items, the subtests with the lowest standardized scores were alternating verbal fluency ($z = -0.63$), working memory ($z = -0.45$), and delayed recall ($z = -0.39$). In contrast, the highest standardized performances were observed in naming ($z = 0.62$), clock copy ($z = 0.45$), and action verbal fluency ($z = 0.31$). Fig. 1 depicts these findings. Given the recognized cognitive heterogeneity in HD, we also performed an exploratory analysis to assess whether distinct phenotypic patterns could be identified within our cohort. To this end, we calculated within–HD-ISS–stage z-scores for PD-CRS subcortical and cortical subscores and screened for participants whose normalized performance deviated significantly ($\geq$1.5 SD below the stage mean), which would suggest a subcortical-predominant, cortical-predominant, or mixed phenotype. This analysis revealed no extreme phenotypes in stages 1 and 2, and only two cases in stage 3 ($\approx$6 %), one with a cortical-predominant and one with a mixed profile. Overall, while variability was greater in subcortical than in cortical subscores, the absence of consistent extreme profiles across stages argues against the existence of clearly differentiated phenotypes in this dataset. For this reason, no further phenotype-specific analyses were conducted.

To identify clinical and behavioral predictors of global cognition, we conducted a multiple linear regression with PD-CRS total score as the dependent variable. Predictors included total scores from the PBAs, age, CAG repeat length, education, CAP score, and UHDRS-TMS. The model was significant, explaining a large proportion of variance in cognition ($R^2 = 0.862$; $F(16,35) = 13.65$; $p < 0.001$). Perseverative behavior was the strongest negative correlate of PD-CRS scores ($B = -4.26$, $p < 0.001$), followed by motor symptom severity ($B = -0.35$, $p = 0.006$). Education showed a positive association ($B = 1.73$, $p = 0.001$). Other PBAs domains, age, CAG repeat length, and CAP score had no significant effects.

PD-CRS scores declined significantly with disease progression [$F(2,49) = 4.29$; $p = 0.019$]. Stage 3 showed lower total scores than stage 1 [$t(41) = 3.08$; $p = 0.004$; $d = 1.30$], and stage 2 was also lower than stage 1 [$t(17) = 4.84$; $p < 0.001$; $d = 2.30$]. Subcortical scores followed a similar pattern [$F(2,49) = 3.84$; $p = 0.027$], with significant reductions in stage 3 and 2 vs stage 1. Cortical scores declined across stages [$F(2,49) = 3.50$; $p = 0.037$], with a significant drop in stage 3 vs stage 1 [$t(41) = 2.50$; $p = 0.017$; $d = 1.06$], but no difference between stages 1 and 2. PD-CRS-based cognitive staging confirmed this gradient. All participants in stage 1 (100 %) were cognitively normal. In stage 2, 4 (44.4 %) met criteria for MCI (PD-CRS$\leq$82) and 1 (11.1 %) for dementia (PD-CRS$\leq$64). In stage 3, 16 (48.5 %) met the MCI threshold and 8 (24.2 %) met dementia criteria.

3.2. Neuroanatomical correlates of PD-CRS

As reported in Fig. 2 and Table 2, Two clusters survived whole-brain family-wise error (FWE) correction at the cluster level. The largest cluster (24,263 voxels; $p < 0.001$, FWE-corrected) encompassed a broad bilateral frontostriatal and limbic-paralimbic network. On the left hemisphere, significant involvement was observed in the anterior and dorsolateral putamen, head of the caudate nucleus, ventral striatum, and both the external and internal segments of the globus pallidus. Extending anteriorly, the cluster reached the subcallosal cortex and orbitofrontal areas, while laterally it engaged the anterior insula to the

Table 1
Clinical and sociodemographic data of the sample.

Mean (SD) & Range						
Variable	Stage 1 Mean (SD)	Stage 1 Range	Stage 2 Mean (SD)	Stage 2 Range	Stage 3 Mean (SD)	Stage 3 Range
Gender	(5/5)	–	(6/3)	–	(14/19)	–
Age (years)	45.2 (8.6)	35–63	46.1 (7.7)	32–60	53.3 (10.8)	26–72
Education (years)	15.9 (3.7)	11–22	14.3 (2.2)	11–18	13.3 (3.8)	7–22
CAG	42.3 (2.3)	39–46	43.4 (1.9)	41–47	44.1 (3.8)	39–56
CAP score	378.5 (62.3)	310–470	442.3 (60.9)	333–526	521.5 (92.4)	373–666
cUHDRS	17.6 (1.4)	15–19	13.5 (1.8)	11–17	7.5 (4.3)	0–16
UHDRS-TMS	2.4 (2.3)	0–7	13.2 (8.7)	2–28	44.7 (19.4)	5–80
TFC	13.0 (0.0)	13–13	12.8 (0.4)	12–13	9.2 (2.5)	4–13
FIS	25.0 (0.0)	25–25	24.8 (0.7)	24–26	19.6 (3.5)	15–29
PD-CRS Total	111.6 (9.9)	99–128	80.6 (15.2)	54–101	73.7 (17.9)	35–117
Cortical score	28.7 (1.3)	27–30	27.6 (3.4)	20–30	26.0 (3.7)	15–30
Subcortical score	82.9 (10.0)	70–98	53.0 (13.1)	34–71	47.7 (15.6)	20–88

CAG: CAG repeat length; CAP score: CAG x AGE product; UHDRS-TMS: Unified Huntington's Disease Rating Scale Total Motor Score; cUHDRS: Composite UHDRS; TFC: Total Functional Capacity; FIS: Functional Independence Score; PD-CRS: Parkinson's Disease – Cognitive Rating Scale.

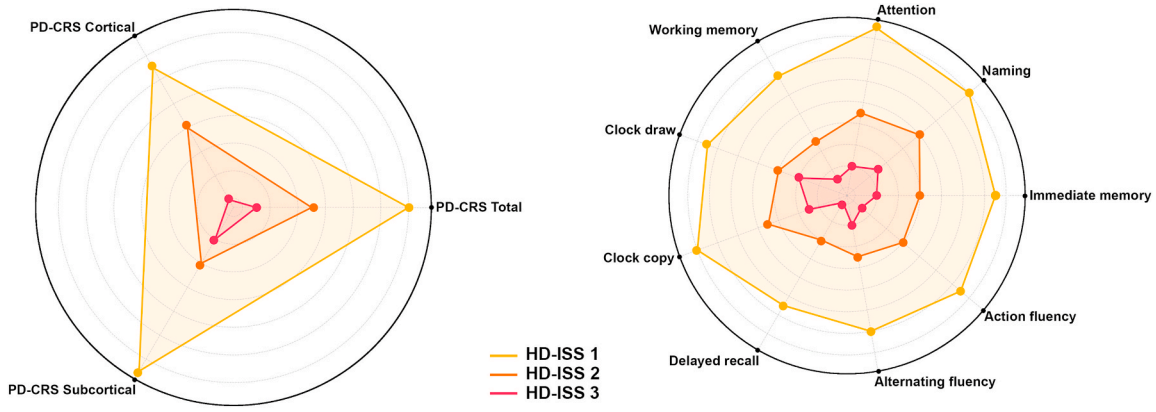

Fig. 1. Distribution of the PD-CRS scores across groups.

anterior putamen. Importantly, this cluster also extended into homologous regions of the right hemisphere. Right-lateralized effects were observed in the ventral striatum, pallidum, and putamen, as well as in paralimbic areas including the anterior insula. The second cluster (9565 voxels; $p < 0.001$, FWE-corrected) was located predominantly in the right posterior parietal and occipital cortices. The more significant effects were found in the superior parietal lobule, angular gyrus, precuneus, and lateral occipital regions, including the parieto-occipital junction and cuneus.

To assess whether the relationship between GMV and cognition was independent of motor and behavioral symptoms, we ran a multiple linear regression across the full sample. The dependent variable was mean GMV across significant VBM-derived ROIs; predictors included UHDRS-TMS and PBA perseveration scores, previously identified as strong cognitive correlates. The model was significant, explaining a moderate proportion of GMV variance ($R^2 = 0.326$, adjusted $R^2 = 0.298$; $F(2,49) = 11.83$; $p < 0.001$). Both predictors contributed: greater motor severity ($B = -0.0104$, $p = 0.002$) and higher perseveration ($B = -0.0323$, $p = 0.012$) were linked to reduced GMV. However, when PD-CRS total scores were added, cognition emerged as the strongest predictor ($B = 0.0038$, $p < 0.001$), indicating a unique association with brain structure beyond motor and behavioral effects.

To investigate whether the structural–cognitive associations varied across disease progression, we repeated the analyses using regional GMV extracted from the VBM-derived fronto-striatal and posterior clusters. Significant effects of HD-ISS stage were observed for both clusters (fronto-striatal: $F(2,45) = 11.37$, $p = 0.0001$; posterior: $F(2,45) = 14.00$, $p = 0.00002$), with substantially reduced volumes in stage 3 compared to stages 1–2. Within-stage regressions, using as predictors the PD-CRS total score, the UHDRS-TMS and the PBAs perseveration scores, the analysis confirmed different contribution patterns across stages. In stage 1, all predictors significantly accounted for GMV variance in the fronto-striatal cluster ($R^2 = 0.92$, $p = 0.004$–0.005), and motor and perseverative symptoms also contributed in the posterior cluster ($R^2 = 0.89$, $p = 0.002$–0.019). In stage 2, no significant associations emerged ($R^2 \leq 0.21$, all $p > 0.62$). In stage 3, the PD-CRS was the most consistent predictor of GMV in both clusters ($R^2 = 0.29$–0.37; $p \leq 0.08$).

3.3. *Associations between regional gray matter volumes and PD-CRS subdomains*

Significant relationships ($p < 0.05$) were found for all subdomains, with particularly strong effects for immediate memory, attention, and verbal fluency. Higher GMV consistently predicted better cognitive performance. Immediate memory was positively associated with GMV in the left striatum ($B = 2.77$, $p < 0.001$, $R^2 = 0.29$), posterior cortex ($B = 0.62$, $p < 0.001$, $R^2 = 0.28$), calcarine cortex ($B = 2.01$, $p = 0.001$, $R^2 = 0.28$), left midtemporal ($B = 2.48$, $p = 0.003$, $R^2 = 0.23$), and left frontal-striatal regions ($B = 1.47$, $p = 0.018$, $R^2 = 0.17$). Attention scores correlated strongly with GMV in the posterior cortex ($B = 1.07$, $R^2 = 0.47$), left striatum ($B = 4.65$, $R^2 = 0.46$), left midtemporal ($B = 4.54$, $R^2 = 0.40$), calcarine cortex ($B = 3.21$, $R^2 = 0.40$), and TPJ ($B = 14.06$, all $p < 0.001$, $R^2 = 0.38$). Copy of a clock performance showed significant associations with GMV in the left striatum ($B = 1.26$, $p = 0.001$), calcarine, TPJ, posterior cortex, and bilateral midtemporal/striatal regions (all $p < 0.02$). Unprompted drawing of a clock was related to GMV in the left striatum ($B = 1.37$, $p = 0.004$), right striatum, calcarine, TPJ, and midtemporal cortex. Working memory was linked to GMV in the right

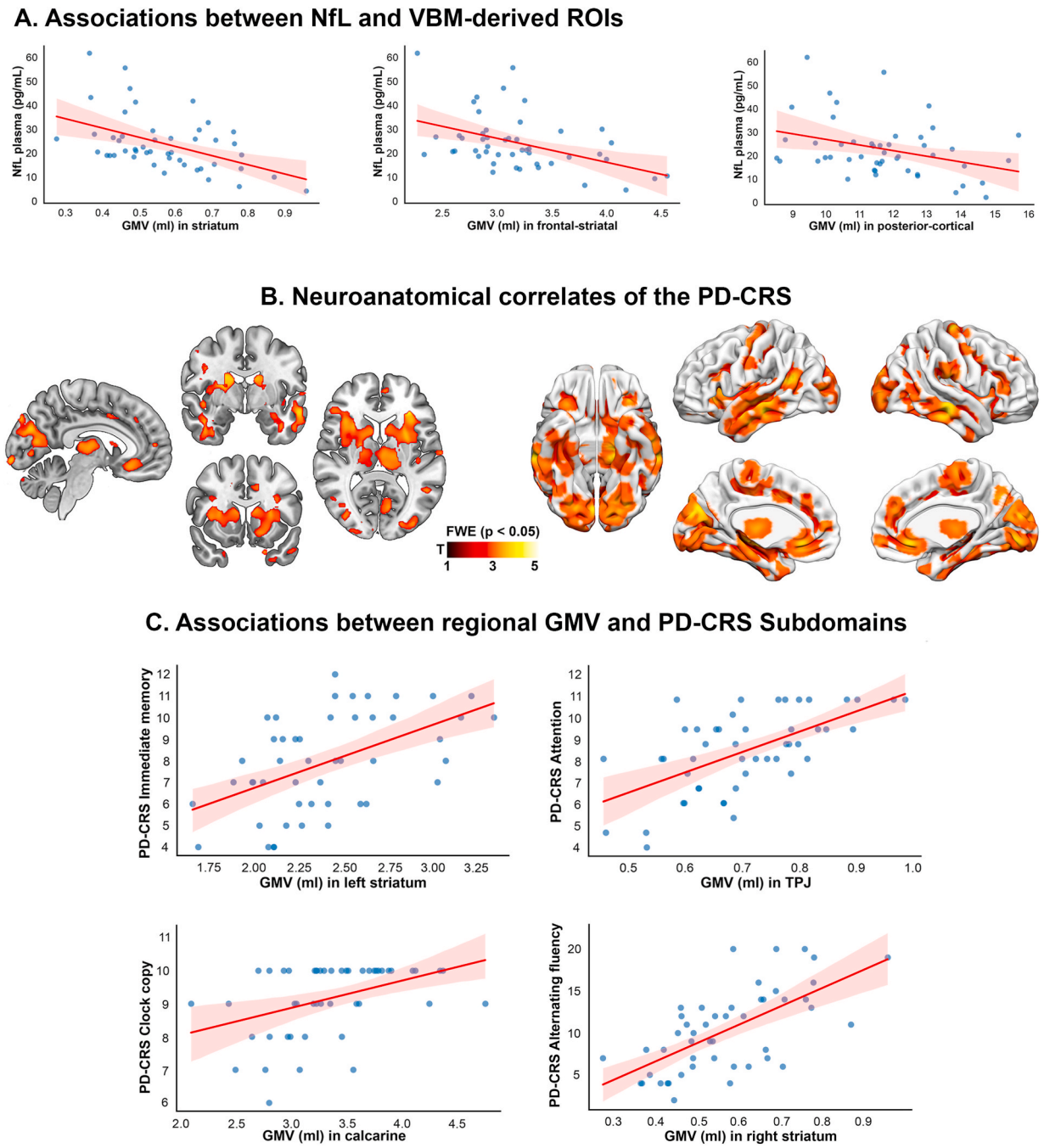

Fig. 2. Neuroimaging results

Section A displays the association between GMV extracted from the VBM-derived clusters and serum NfL concentrations. Each dot represents an individual participant. Regression lines indicate the direction and strength of the association, with shaded areas showing the 95 % confidence interval. Higher NfL levels reflect increased neuroaxonal damage and are associated with lower GMV in these regions.

Section B illustrates the spatial distribution of GMV reductions associated with poorer PD-CRS total performance. Statistical parametric maps are shown on the MNI template in neurological convention, with warmer colors indicating stronger negative associations (cluster-level FWE-corrected $p < 0.05$).

Section C depicts representative associations between GMV in selected regions and performance on individual PD-CRS subtests, highlighting domain-specific vulnerability. Higher scores indicate better cognitive performance. Axes, slopes and confidence intervals are reported to facilitate interpretation of effect sizes.

striatum ($B = 6.08$, $p < 0.001$), as well as the posterior cortex, left striatum, and left midtemporal regions. Verbal fluency (alternating and action) showed widespread associations across nearly all ROIs. Alternating fluency was linked to right striatum, left striatum, posterior cortex, calcarine, TPJ, and midtemporal cortex (all $p < 0.005$). Action fluency was most strongly related to right striatum ($B = 28.31$, $p < 0.001$), with additional associations in posterior cortex, calcarine, frontal-striatal, and TPJ regions. Recognition memory correlated with GMV in right striatum ($B = 9.53$, $p < 0.001$), left striatum, posterior cortex, and calcarine cortex. Naming was moderately associated with posterior cortex ($B = 0.35$, $p = 0.033$), bilateral striatum, and calcarine cortex (all $p < 0.04$). Across all models, age was not a significant covariate.

Table 2
GMV correlates of the PD-CRS.

Anatomical Label	MNI (X,Y,Z)	T value	Hemisphere	Cluster
Putamen anterior	−30, −15, −5	4.78	Left	1
Occipital cortex/Lingual gyrus	35, −75, 5	4.32	Right	2
Angular gyrus/Inferior parietal lobule	−33, −63, 24	4.25	Left	2
Cuneus/Occipital pole	20, −90, 31	4.21	Right	2
Superior temporal gyrus/TPJ	−54, −30, 31	4.12	Left	1
Precuneus/Posterior cingulate cortex	10, −48, 42	3.98	Right	2
Angular gyrus/Inferior parietal	−31, −64, 20	3.92	Left	2
Middle occipital gyrus	51, −75, 31	3.90	Right	2
Putamen	−27, −24, −9	3.90	Left	1
Lateral occipital cortex	45, −69, 29	3.85	Right	2
Ventral pallidum/Sub-lenticular region	−36, −35, −11	3.85	Left	1
Superior parietal lobule	21, −60, 50	3.81	Right	2
Globus pallidus interna	−24, −6, −12	3.78	Left	1
Angular gyrus/Posterior STG	36, −65, 20	3.73	Right	2

3.4. Association between plasma neurofilament levels and global cognitive function (PD-CRS)

Lower cognitive performance was significantly associated with higher NfL levels ($B = -0.153$, $p = 0.048$; $R^2 = 0.076$). This association remained significant after adjusting for age ($B = -0.165$, $p = 0.032$), while age alone was not a significant predictor ($B = -0.255$, $p = 0.107$). The age-adjusted model explained 12.4 % of the variance in NfL ($R^2 = 0.124$).

3.5. Association between plasma neurofilament levels and regional gray matter volume

Results consistently showed inverse associations between GMV and NfL, indicating that greater atrophy is linked to higher neurodegeneration. Strongest effects were observed in the left frontal-striatal region ($B = -11.38$, $p < 0.001$) and posterior cortex ($B = -2.77$, $p = 0.004$), both surviving age correction. Age remained significant in most models but with smaller effects than GMV. Regression coefficients (B) and p-values are summarized in Table 3.

4. Discussion

The present study investigated the neuroanatomical correlates of global cognitive functioning in HD using the PD-CRS, a cognitive screening instrument originally validated in PD and recently explored in HD (Horta-Barba et al., 2023; Martinez-Horta et al., 2020a). Our findings support the PD-CRS as a sensitive and clinically relevant tool for detecting cognitive impairment in HD, and demonstrate its robust association with GMV across a distributed frontostriatal, limbic, and parietal-occipital network. However, further validation of the PD-CRS in independent HD cohorts will be essential to strengthen its generalizability.

Table 3
Association between plasma neurofilament and GMV.

ROIs	B (GMV)	p (GMV)	B (Age)	p (Age)	R (Ross and Tabrizi, 2011)
Calcarine	−8.50	0.007	−0.38	0.017	0.204
Left Frontal-striatal	−11.38	0.000	−0.36	0.013	0.301
Left mid temporal	−9.66	0.032	−0.33	0.040	0.153
Left Striatum	−11.37	0.007	−0.35	0.026	0.200
Parietal-occipital	−2.77	0.004	−0.36	0.019	0.222
Right mid temporal	−13.16	0.182	−0.35	0.041	0.098
Right striatum	−42.48	0.000	−0.36	0.013	0.325
TPJ	−32.92	0.021	−0.37	0.022	0.167

Clinically, cognitive impairment was highly prevalent in our cohort, with 58 % of participants meeting criteria for MCI and 19 % for dementia, based on validated PD-CRS thresholds (Martinez-Horta et al., 2020a). These rates increased consistently across HD-ISS stages. Importantly, all participants in stage 1 displayed preserved cognition, supporting the construct validity of the PD-CRS as a staging tool even in early or premanifest disease. At the item level, performance varied by cognitive domain, with executive-attentional tasks, particularly sustained attention and alternating verbal fluency, emerging as the most sensitive to disease progression.

VBM analyses identified two large clusters where GMV significantly correlated with global PD-CRS scores. The first encompassed a bilateral frontostriatal and paralimbic network (Alexander et al., 1986; Haber and Knutson, 2010; Menon and Uddin, 2010). These regions are among the earliest and more consistently affected structures in HD (Ross et al., 2014; Tabrizi et al., 2009, 2011). The involvement of orbitofrontal and insular cortices, as well as subcallosal and ventral striatal regions, underscores the progressive engagement of limbic-prefrontal circuits as the disease advances (Enzi et al., 2012; Martinez-Horta et al., 2018, 2021). These structures subserve a wide range of cognitive domains that are prominently impaired in HD and that are targeted by the PD-CRS. The caudate and putamen play a central role in action selection, procedural memory, and attentional gating, while the globus pallidus and ventral striatum contribute to motivation, decision-making, and cognitive flexibility (Haber and Knutson, 2010; Yin and Knowlton, 2006; Grahn et al., 2008). The anterior insula is involved in salience detection and the integration of cognitive and affective information, and the subcallosal area has been linked to mood and cognitive control (Menon and Uddin, 2010). Through its diverse subtests, the PD-CRS assesses many of these domains, such as attention, working memory, and verbal fluency, making it well suited to detect dysfunction across this network.

The second cluster, centered in the right posterior parietal and occipital cortex, involved regions supporting visuospatial integration and cognitive flexibility (Kawasaki et al., 2008; Seghier, 2013; Cavanna and Trimble, 2006; Whitlock, 2017). Degeneration in posterior brain regions, particularly parietal and occipital cortices, was historically neglected in early descriptions of HD. However, accumulating evidence demonstrates that structural alterations in these regions emerge well before clinical diagnosis, with cortical thinning detectable even in prodromal and premanifest individuals (Rosas et al., 2008; Tabrizi et al., 2009; Martinez-Horta et al., 2024; Nopoulos et al., 2010). Our results align with this literature by showing that PD-CRS performance is significantly associated with GMV in parietal-occipital regions, suggesting that this scale captures early, spatially distributed cortical involvement.

To better understand the factors influencing cognitive performance, we ran a multiple regression with PD-CRS total scores as the outcome. The model explained a large proportion of variance, identifying perseverative behavior, motor severity, and education as significant predictors. These findings highlight the combined association between cognitive reserve, motor decline, and psychiatric symptoms with cognition in HD, although with the present cross-sectional data we cannot attribute a specific directionality or infer a clear causal relationship beyond correlation. We then tested whether motor and behavioral symptoms could account for GMV reductions in PD-CRS-related regions. Without cognitive scores, UHDRS-TMS and PBA perseveration were significantly linked to GMV. However, when PD-CRS was added, it became the strongest predictor, suggesting that GMV loss reflects cognitive decline beyond motor or behavioral dysfunction. It

should also be acknowledged that PBA-s scores were particularly low in our cohort, which may reflect cohort-specific or care-related factors that attenuate the expression of neuropsychiatric symptoms. In other regions or healthcare settings, these values might differ substantially, and thus the associations we observed are likely not fully generalizable and should be interpreted as dependent, at least in part, on the behavioral profile of the studied sample.

Importantly, stage-stratified analyses revealed that the expression of these structure–function relationships varies along disease progression. While multiple clinical dimensions (cognitive, motor and behavioural) were related to GMV in early disease, cognition became the principal correlate in advanced stages, in line with the dominant impact of neurodegeneration on daily functioning at later phases. The absence of robust associations in stage 2 likely reflects reduced variability once symptoms are clinically established, limiting sensitivity to detect differential contributions. Together, these results support the role of PD-CRS as a biologically meaningful index of neurodegeneration over the HD progression continuum.

Beyond global cognition, we also examined how specific PD-CRS subdomains mapped onto regional gray matter volumes. Results demonstrated clear topographic organization: fronto-striatal regions were preferentially associated with verbal fluency and working memory, posterior cortices with visuospatial functions (e.g., clock copy), and temporo-parietal junctions with attentional processing. These domain-specific anatomical associations validate the internal structure of the PD-CRS and reinforce its relevance for tracking both focal and diffuse cognitive deterioration. Importantly, age was not a significant covariate in any of the subdomain analyses, further highlighting the specificity of these associations.

At the biomarker level, plasma NfL levels were significantly associated with PD-CRS scores, even after adjusting for age, indicating that the PD-CRS reflects neurodegeneration beyond structural atrophy (Byrne et al., 2017; Parkin et al., 2024). NfL also showed inverse correlations with GMV in key regions, particularly the left frontal-striatal and posterior cortices, mirroring PD-CRS-related structural changes. These results support the PD-CRS as a meaningful cognitive marker of both brain pathology and fluid biomarkers of disease burden and build on and extend our previous works validating the PD-CRS in HD (Horta-Barba et al., 2023; Martinez-Horta et al., 2020a).

Consistent with prior findings, we show that both total PD-CRS scores and specific subdomains are significantly associated with gray matter volume in posterior parietal and occipital cortices (Martinez-Horta et al., 2020a, 2020b). These associations remained significant after controlling for age and motor severity, highlighting the PD-CRS specificity in capturing neural correlates of cognitive decline. Across independent samples and complementary methods, evidence converges to support the PD-CRS as both a clinically valid staging tool and a sensitive marker of widespread neurodegeneration in HD. Beyond these findings that reinforce the strength and utility of the PD-CRS, other factors further enhance its applicability. One notable advantage is its availability in multiple validated translations, including languages spoken in Western Europe, Asia, and Latin America, supporting its global use in diverse clinical and research contexts.

Despite these strengths, several limitations should be acknowledged. First, while our sample spanned a wide range of disease stages, it remains cross-sectional in nature, precluding conclusions about the temporal progression of structural-cognitive relationships. Longitudinal studies will be essential to establish whether PD-CRS scores track within-subject changes in brain volume over time. Second, although the PD-CRS captures multiple cognitive domains, it remains a screening tool and does not replace comprehensive neuropsychological testing. In our stage 1 cohort, and while participants were classified as cognitively normal according to PD-CRS normative data, this does not preclude the possibility that they might perform differently from healthy controls in a direct comparison. Future studies with larger samples of stage 1 participants, appropriate control groups, and longitudinal designs will be needed to determine whether the PD-CRS can detect such subtle early differences and to further establish its sensitivity in premanifest and early disease phases. Moreover, the relatively small sample size in HD-ISS stage 2, combined with within-group heterogeneity, likely reduced statistical power and may have limited our ability to detect stage-specific associations and stage-wise analyses were exploratory and sample sizes, especially in stages 1–2, constrain statistical power; therefore, these results should be interpreted with caution pending replication in larger stratified cohorts.

Overall, this study provides robust evidence that the PD-CRS is a neuroanatomically grounded, clinically sensitive tool for assessing cognition in HD, also capturing disease-related structural changes across a broad network of functionally relevant brain regions. These findings, together with previous work, highlight the value of further investigating the potential role of the PD-CRS for disease monitoring and as an outcome measure in clinical trials in Huntington's disease, and underscore the importance of anatomically informed cognitive assessment strategies in neurodegenerative disorders.

CRediT authorship contribution statement

Saul Martinez-Horta: Writing – review & editing, Writing – original draft, Visualization, Validation, Resources, Project administration, Methodology, Investigation, Funding acquisition, Formal analysis, Data curation, Conceptualization. **Arnau Puig-Davi:** Writing – original draft, Project administration, Methodology, Investigation, Formal analysis, Data curation. **Frederic Sampedro:** Writing – original draft, Methodology, Investigation, Formal analysis. **Jesús Pérez-Pérez:** Writing – review & editing, Writing – original draft, Project administration, Investigation, Funding acquisition, Formal analysis. **Carla Franch-Martí:** Writing – original draft, Resources, Project administration, Methodology, Investigation. **Gonzalo Olmedo-Saura:** Writing – original draft, Project administration, Investigation, Formal analysis. **Elisa Rivas-Asensio:** Writing – original draft, Methodology, Investigation, Formal analysis. **Anna Vazquez-Oliver:** Writing – original draft, Software, Methodology, Investigation. **Laura Pérez-Carasol:** Writing – original draft, Validation, Supervision, Methodology, Investigation, Formal analysis. **Andrea Horta-Barba:** Writing – original draft, Project administration, Methodology, Investigation. **Javier Pagonabarraga:** Writing – review & editing, Writing – original draft, Resources, Project administration, Funding acquisition. **Jaime Kulisevsky:** Writing – review & editing, Writing – original draft, Validation, Supervision, Resources, Funding acquisition.

Ethical compliance statement

This study was approved by the Institutional Review Board of the Hospital de la Santa Creu i Sant Pau. Written informed consent was obtained from all patients prior to their participation and was properly documented in accordance with institutional policies. We confirm that we have read the Journal's position on issues involved in ethical publication and affirm that this work is consistent with those guidelines.

Declaration of competing interest

The authors declare the following financial interests/personal relationships which may be considered as potential competing interests: Saul Martinez-Horta reports financial support was provided by Carlos III Health Institute. If there are other authors, they declare that they have no known competing financial interests or personal relationships that could have appeared to influence the work reported in this paper.

Acknowledgment

The authors wish to express their gratitude to all those impacted by Huntington's disease who actively participated in this study. This study

was funde by a grant from ISCIII (PI21/01758), Fondos FEDER.

Appendix A. Supplementary data

Supplementary data to this article can be found online at https://doi.org/10.1016/j.ynirp.2025.100311.

Data availability

Data will be made available on request.

References

Adanyeguh, I.M., Branzoli, F., Delorme, C., et al., 2021. Multiparametric characterization of white matter alterations in early stage Huntington disease. Sci. Rep. 11 (1), 13101.

Alexander, G.E., DeLong, M.R., Strick, P.L., 1986. Parallel organization of functionally segregated circuits linking basal ganglia and cortex. Annu. Rev. Neurosci. 9, 357–381.

Begeti, F., Tan, A.Y., Cummins, G.A., et al., 2013. The Addenbrooke's cognitive examination-revised accurately detects cognitive decline in Huntington's disease. J. Neurol. 260 (11), 2777–2785.

Byrne, L.M., Rodrigues, F.B., Blennow, K., et al., 2017. Neurofilament light protein in blood as a potential biomarker of neurodegeneration in Huntington's disease: a retrospective cohort analysis. Lancet Neurol. 16 (8), 601–609.

Callaghan, J., Stopford, C., Arran, N., et al., 2015. Reliability and factor structure of the short problem behaviors assessment for Huntington's disease (PBA-s) in the TRACK-HD and REGISTRY studies. J. Neuropsychiatry Clin. Neurosci. 27 (1), 59–64.

Cavanna, A.E., Trimble, M.R., 2006. The precuneus: a review of its functional anatomy and behavioural correlates. Brain 129 (Pt 3), 564–583.

Enzi, B., Edel, M.A., Lissek, S., et al., 2012. Altered ventral striatal activation during reward and punishment processing in premanifest Huntington's disease: a functional magnetic resonance study. Exp. Neurol. 235 (1), 256–264.

Folstein, M.F., Folstein, S.E., McHugh, P.R., 1975. "Mini-mental state". A practical method for grading the cognitive state of patients for the clinician. J. Psychiatr. Res. 12 (3), 189–198.

Grahn, J.A., Parkinson, J.A., Owen, A.M., 2008. The cognitive functions of the caudate nucleus. Prog. Neurobiol. 86 (3), 141–155.

Group, H.S., 1996. Unified Huntington's Disease rating scale: reliability and consistency. Huntington study group. Mov. Disord. 11 (2), 136–142.

Haber, S.N., Knutson, B., 2010. The reward circuit: linking primate anatomy and human imaging. Neuropsychopharmacology 35 (1), 4–26.

Horta-Barba, A., Martinez-Horta, S., Perez-Perez, J., et al., 2023. Measuring cognitive impairment and monitoring cognitive decline in Huntington's disease: a comparison of assessment instruments. J. Neurol. 270 (11), 5408–5417.

Kawasaki, M., Watanabe, M., Okuda, J., Sakagami, M., Aihara, K., 2008. Human posterior parietal cortex maintains color, shape and motion in visual short-term memory. Brain Res. 1213, 91–97.

Litvan, I., Goldman, J.G., Troster, A.I., et al., 2012. Diagnostic criteria for mild cognitive impairment in Parkinson's disease: movement disorder society task force guidelines. Mov. Disord. 27 (3), 349–356.

Marras, C., Troster, A.I., Kulisevsky, J., Stebbins, G.T., 2014. The tools of the trade: a state of the art "How to Assess Cognition" in the patient with Parkinson's disease. Mov. Disord. 29 (5), 584–596.

Martinez-Horta, S., Perez-Perez, J., Sampedro, F., et al., 2018. Structural and metabolic brain correlates of apathy in Huntington's disease. Mov. Disord. 33 (7), 1151–1159.

Martinez-Horta, S., Horta-Barba, A., Perez-Perez, J., et al., 2020a. Utility of the Parkinson's disease-cognitive rating scale for the screening of global cognitive status in Huntington's disease. J. Neurol. 267 (5), 1527–1535.

Martinez-Horta, S., Sampedro, F., Horta-Barba, A., et al., 2020b. Structural brain correlates of dementia in Huntington's disease. Neuroimage Clin 28, 102415.

Martinez-Horta, S., Sampedro, F., Horta-Barba, A., et al., 2021. Structural brain correlates of irritability and aggression in early manifest Huntington's disease. Brain Imaging Behav 15 (1), 107–113.

Martinez-Horta, S., Perez-Perez, J., Oltra-Cucarella, J., et al., 2023. Divergent cognitive trajectories in early stage Huntington's disease: a 3-year longitudinal study. Eur. J. Neurol. 30 (7), 1871–1879.

Martinez-Horta, S., Perez-Perez, J., Perez-Gonzalez, R., et al., 2024. Cognitive phenotype and neurodegeneration associated with Tau in Huntington's disease. Ann Clin Transl Neurol 11 (5), 1160–1171.

Menon, V., Uddin, L.Q., 2010. Saliency, switching, attention and control: a network model of insula function. Brain Struct. Funct. 214 (5–6), 655–667.

Mestre, T.A., Bachoud-Levi, A.C., Marinus, J., et al., 2018. Rating scales for cognition in Huntington's disease: critique and recommendations. Mov. Disord. 33 (2), 187–195.

Nopoulos, P.C., Aylward, E.H., Ross, C.A., et al., 2010. Cerebral cortex structure in prodromal Huntington disease. Neurobiol. Dis. 40 (3), 544–554.

Pagonabarraga, J., Kulisevsky, J., Llebaria, G., Garcia-Sanchez, C., Pascual-Sedano, B., Gironell, A., 2008. Parkinson's disease-cognitive rating scale: a new cognitive scale specific for Parkinson's disease. Mov. Disord. 23 (7), 998–1005.

Parkin, G.M., Thomas, E.A., Corey-Bloom, J., 2024. Mapping neurodegeneration across the Huntington's disease spectrum: a five-year longitudinal analysis of plasma neurofilament light. EBioMedicine 104, 105173.

Reber, J., Hwang, K., Bowren, M., et al., 2021. Cognitive impairment after focal brain lesions is better predicted by damage to structural than functional network hubs. Proc. Natl. Acad. Sci. U. S. A. 118 (19).

Rosas, H.D., Salat, D.H., Lee, S.Y., et al., 2008. Cerebral cortex and the clinical expression of Huntington's disease: complexity and heterogeneity. Brain 131 (Pt 4), 1057–1068.

Rosca, E.C., Simu, M., 2022. Montreal cognitive assessment for evaluating cognitive impairment in Huntington's disease: a systematic review. CNS Spectr. 27 (1), 27–45.

Rosen, W.G., Mohs, R.C., Davis, K.L., 1984. A new rating scale for Alzheimer's disease. Am. J. Psychiatr. 141 (11), 1356–1364.

Ross, C.A., Tabrizi, S.J., 2011. Huntington's disease: from molecular pathogenesis to clinical treatment. Lancet Neurol. 10 (1), 83–98.

Ross, C.A., Aylward, E.H., Wild, E.J., et al., 2014. Huntington disease: natural history, biomarkers and prospects for therapeutics. Nat. Rev. Neurol. 10 (4), 204–216.

Rosser, A.E., Hodges, J.R., 1994. The Dementia rating scale in Alzheimer's disease, Huntington's disease and progressive supranuclear palsy. J. Neurol. 241 (9), 531–536.

Schobel, S.A., Palermo, G., Auinger, P., et al., 2017. Motor, cognitive, and functional declines contribute to a single progressive factor in early HD. Neurology 89 (24), 2495–2502.

Seghier, M.L., 2013. The angular gyrus: multiple functions and multiple subdivisions. Neuroscientist 19 (1), 43–61.

Sierra, L.A., Ullman, C.J., Baselga-Garriga, C., Pandeya, S.R., Frank, S.A., Laganiere, S., 2023. Prevalence of neurocognitive disorder in Huntington's disease using the Enroll-HD dataset. Front. Neurol. 14, 1198145.

Snowden, J.S., 2017. The neuropsychology of Huntington's Disease. Arch. Clin. Neuropsychol. 32 (7), 876–887.

Stout, J.C., Queller, S., Baker, K.N., et al., 2014. HD-CAB: a cognitive assessment battery for clinical trials in Huntington's disease 1,2,3. Mov. Disord. 29 (10), 1281–1288.

Tabrizi, S.J., Langbehn, D.R., Leavitt, B.R., et al., 2009. Biological and clinical manifestations of Huntington's disease in the longitudinal TRACK-HD study: cross-sectional analysis of baseline data. Lancet Neurol. 8 (9), 791–801.

Tabrizi, S.J., Scahill, R.I., Durr, A., et al., 2011. Biological and clinical changes in premanifest and early stage Huntington's disease in the TRACK-HD study: the 12-month longitudinal analysis. Lancet Neurol. 10 (1), 31–42.

Tabrizi, S.J., Reilmann, R., Roos, R.A., et al., 2012. Potential endpoints for clinical trials in premanifest and early Huntington's disease in the TRACK-HD study: analysis of 24 month observational data. Lancet Neurol. 11 (1), 42–53.

Tabrizi, S.J., Schobel, S., Gantman, E.C., et al., 2022. A biological classification of Huntington's disease: the Integrated staging system. Lancet Neurol. 21 (7), 632–644.

Warner, J.H., Long, J.D., Mills, J.A., et al., 2022. Standardizing the CAP score in Huntington's disease by predicting age-at-onset. J Huntingtons Dis 11 (2), 153–171.

Whitlock, J.R., 2017. Posterior parietal cortex. Curr. Biol. 27 (14), R691–R695.

Yin, H.H., Knowlton, B.J., 2006. The role of the basal ganglia in habit formation. Nat. Rev. Neurosci. 7 (6), 464–476.